CP845, *Shock Compression of Condensed Matter - 2005,*
edited by M. D. Furnish, M. Elert, T. P. Russell, and C. T. White


# POST-SHOCK TEMPERATURE MEASUREMENTS OF ALUMINUM

**A. Seifter[1], S. T. Stewart[2], M. R. Furlanetto[1], G. B. Kennedy[2], J. R. Payton[1], and A. W. Obst[1]**

[1] *University of California, Los Alamos National Laboratory, Physics Division, P-23, Los Alamos, NM 87545*
[2] *Department of Earth and Planetary Sciences, Harvard University, 20 Oxford Street, Cambridge MA 02138*

**Abstract.** Post-shock temperature is an important quantity in shock physics experiments for constraining the dynamic equations of state of materials. A high-speed, infrared, multi-wavelength pyrometer has been developed at Los Alamos National Laboratory (LANL) for measurements in the temperature range from 400 to 1200 K. With customized front end optics, permitting concurrent VISAR measurements in the same optical path, validation experiments on aluminum have been conducted at the new Shock Compression Laboratory at Harvard University. Under <1 millitorr vacuum, a post-shock temperature of 495 K ± 30 K was recorded from a polished free surface of aluminum 2024-T4 subject to a peak shock pressure of 34.8±0.8 GPa, in excellent agreement with the equation of state and previous experiments.

**Keywords:** Pyrometry, infrared optics, post-shock temperatures, aluminum, equations of state
**PACS:** 62.50.+p, 65.40.-b, 83.85.Ei, 07.20.Ka

## INTRODUCTION

Post-shock temperature measurements of metals provide strong constraints on their equations of state (EOS). In general, shock temperature data of condensed matter are necessary to investigate a wide range of programmatic as well as natural phenomena. In fact, since the pioneering work of Raikes and Ahrens [1], very little work has been done on metals in the infrared wavelength regime.

Recent developments in experimental methods to measure peak shock temperatures in metals will significantly improve EOS models. Free-surface pyrometry is a powerful tool to both validate and complement new dynamic volume-temperature measurements, such as neutron resonance spectroscopy (NRS), which makes use of Doppler broadening of neutron resonances under shock heating. In a recent study of shocked molybdenum using the NRS technique, the observed peak temperature was about 200 K higher than the calculated temperature based on current models for the equation of state [2].

In a collaborative effort between LANL and the Harvard Shock Compression Laboratory, we are conducting a study of post-shock temperatures of rocks, minerals, and metals, including molybdenum. One of our goals is to provide additional data to resolve the discrepancy between the NRS measurements and the theoretical equation of state for molybdenum. Here we present results of experiments on aluminum to validate our methods using the new LANL 4-channel near-infrared (NIR) pyrometer. We also discuss the experimental and sample preparation methods necessary for accurate free-surface measurements.

## EXPERIMENTAL TECHNIQUE

Experiments were conducted on the 40-mm powder gun at Harvard, which is capable of

launching flyer plates up to a velocity of 2.7 km/s [3]. Figure 1 presents a plan view of the experimental setup within the target chamber. The barrel and the target chamber can be evacuated to below 100 millitorr pressure. However, under such vacuum, the remaining air is shocked to high temperature upon shock breakout from the rear of the sample, preventing direct observation of the cooler free surface temperature of the sample. Hence, the metal sample doubles as the front plate for a small aluminum vacuum chamber, capable of pressures below 1 millitorr, with o-ring seals on the sample and rear 3-mm $CaF_2$ window. To further reduce any air shock, the sample vacuum chamber was purged with helium several times. Under vacuum below 1 millitorr and sample shock pressures of ~35 GPa, no air shock was observed.

The sample vacuum chamber is mounted to a delrin plate with three screws that provide tilt adjustment for alignment to the barrel using a barrel-aligned laser system. The projectile velocity was calculated from the extinction of four cross barrel lasers separated by 15 mm, permitting measurements to 0.1% accuracy. The tilt of the flyer plate is monitored by four shorting pins mounted to the impact face of the sample vacuum chamber.

The thermally-emitted light from a ~4-mm diameter area on the downrange face of the sample is collimated by means of a 2-inch diameter, 2-inch focal length, 90 degree off-axis parabolic (OAP) mirror. The light is passed out of the target chamber through a composite 3-inch diameter window, consisting of a 12.7-mm thick sapphire window protected from debris by a 6-mm thick $CaF_2$ window. The entire light path is protected from muzzle flash by a black nylon baffle.

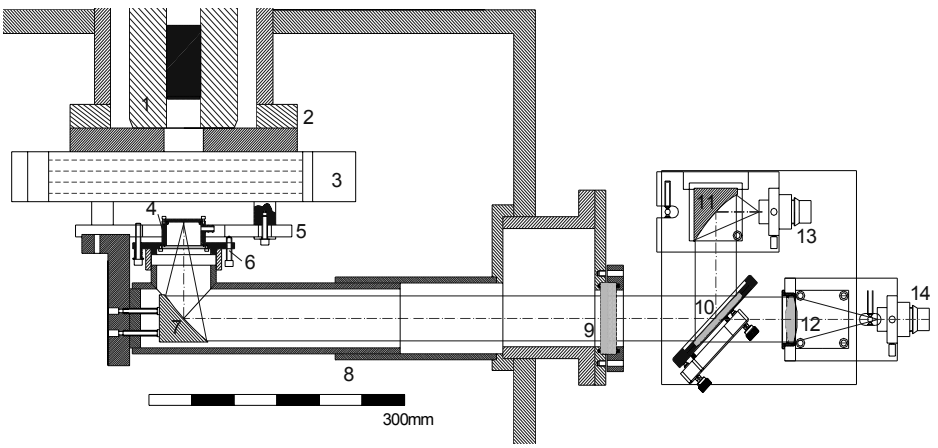


**FIGURE 1.** Plan view of the experimental setup for simultaneous temperature and velocity measurement on the Harvard 40-mm powder gun: 1, gun barrel; 2, muzzle flange; 3, muzzle laser system; 4, sample vacuum chamber; 5, sample vacuum chamber mounting plate; 6, target alignment system; 7, OAP mirror; 8, light baffle; 9, $CaF_2$ and sapphire windows; 10, dichroic beam splitter; 11, OAP mirror; 12, BK7 lens; 13, NIR, and 14, visible fiber chuck holders.

Outside the target chamber, collimated thermally-emitted light above 1200 nm wavelength is reflected by means of a dichroic beamsplitter onto an OAP mirror and focused onto a 1 mm diameter chalcogenide infrared fiber. The fiber delivers the NIR light into the LANL high-speed near-infrared pyrometer. The light is collimated by a 1-inch diameter, 1-inch focal length broadband (1 to 6 μm), antireflective-coated ZnSe lens. Wavelengths below 2100 nm are reflected by a dichroic beamsplitter onto a bandpass filter centered at 1800 nm and then focused by another ZnSe lens onto the 1-mm diameter active area of the liquid-nitrogen cooled InSb detector. This progression is repeated to the other three detectors, as depicted in Figure 2. The detector signals are amplified and recorded by 12-bit, high-speed (400 MS/s, 100 MHz analog bandwidth) digitizers. The temporal resolution of the pyrometer is ~17 ns. The central wavelengths of the four channels are 1.8,

2.3, 3.5 and 4.8 μm. The respective full width at half maximum bandwidths are 298 nm, 393 nm, 536 nm and 903 nm. The pyrometer optics and electronics are housed in an electromagnetically-shielded box.

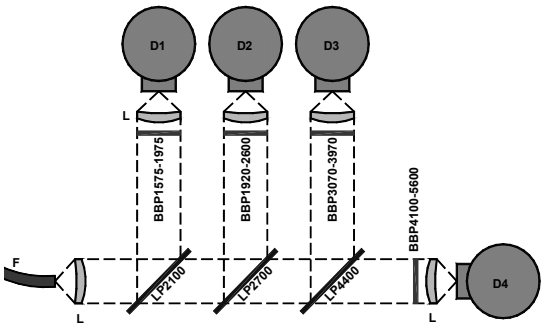


**FIGURE 2.** The optical setup of the pyrometer: D, LN dewars with InSb detectors; L, ZnSe lenses (1" dia., 1" FL); F, chalcogenide fiber; BP, bandpass filter; LP, dichroic beamsplitter.

The radiance temperature (i.e., assuming emissivity of 1) at each wavelength is determined by blackbody calibration. Converting radiance temperature to true temperature requires the normal spectral emissivity at each wavelength. However, emissivity cannot be measured readily under shock conditions, and it is dependent on temperature, wavelength, and surface properties. Therefore, conservative estimates for the upper and lower values for the emissivity are applied to derive a lower and upper limit for the true temperature at each wavelength. The final true temperature and error estimates are derived from the overlapping temperature range between the four channels. For more information on pyrometry in general, see reference 4.

The optical system is shared with a velocity interferometer system for any reflector (VISAR). The VISAR laser delivery and return fiber consists of a bundle of eight 55-μm core diameter fibers. The central fiber delivers 532 nm laser light, and the surrounding seven fibers collect the light reflected from the target. The incident laser light is collimated by a 2-inch diameter, 4-inch focal length BK7 lens with an antireflective coating at the laser wavelength. The dichroic beamsplitter is 95% transparent to the VISAR light. Hence, the OAP mirror behind the target both focuses the incident laser light onto the sample and collimates the reflected laser light. The reflected and collimated VISAR light passes through the dichroic beamsplitter and is focused onto the seven collecting fibers by the same BK7 lens used to collimate the incident light.

## RESULTS

We present results from two experiments on aluminum 2024-T4 with different surface finishes. The samples had a nominal diameter of 43 mm, a nominal thickness of 3.1 mm, and an Archimedean bulk density of 2.783±0.002 kg/m$^3$. The observed sample surfaces had measured root mean square roughness of 726.80 nm for shot #028 (15 micron diamond grit polish) and 52.97 nm (58 nm alumina powder polish) for shot #029. Peak shock pressures of 34.8±0.7 GPa and 34.2±0.4 GPa, respectively, were generated by a 3×34 mm molybdenum flyer plate impacting at 2.27 and 2.24 km/s. Peak pressures were calculated from the impedance match solution using the measured impact velocity and Hugoniots for molybdenum and aluminum 2024-T4 and verified by the measured free surface velocity.

Figure 3 presents the true temperature and free-surface velocity from the aluminum experiments. The free-surface temperature for shot #028, assuming lower and upper limits for the normal spectral emissivity in each channel of 0.1 and 0.5 [1], is 810 K ± 40 K (Fig. 3A). In both experiments, all four pyrometer channels recorded overlapping true temperatures, and we infer that the thermal emission is dominated by a free surface at a nearly constant temperature.

In Fig. 3A, at shock breakout there is a temperature peak of 850 K which decays within 600 ns. A similar temperature spike is seen in previous post-shock temperature measurements on metals and minerals [1, 5]. Possible mechanisms for the temperature spike are described in more detail in reference 5. On the rougher surface sample, the post-shock temperature is about 300 K higher than the temperature reported in the literature for the same material and approximately the same Hugoniot pressure [1].

In the smoother surface sample, the free-surface temperature was 495 K ± 30 K (Fig. 3B).

In this experiment, there was no temperature spike present at the time of shock breakout. The post-shock temperature from shot #029 agrees very well with data from the literature [1], as well as with the equation of state for Al 2024-T4 [6].

The different post-shock temperatures are related to the surface roughness. The rougher free surface may generate micro-jets at temperatures higher than the ideal post-shock temperature. To investigate this hypothesis, we conducted numerical simulations using the shock physics code CTH [7] to determine the free-surface post-shock temperature from a smooth surface and a surface with many valleys. Peak temperatures from the rough and smooth surfaces are in excellent agreement with the data (Fig. 3).

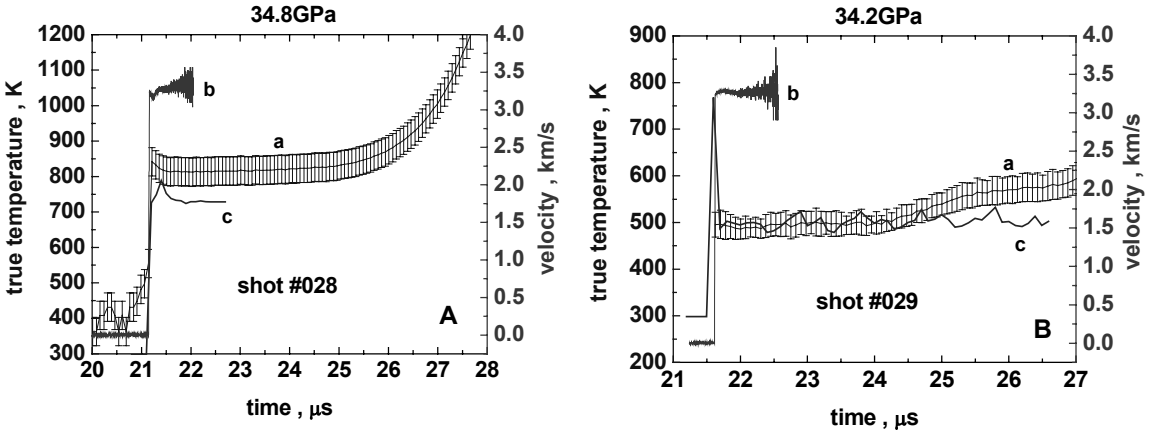


**FIGURE 3.** True temperature (a) and free-surface velocity (b) measurements as well as CTH simulations of free-surface temperatures (c) on rough (A) and polished (B) aluminum 2024-T4.

## CONCLUSIONS

Experiments on aluminum have validated the suitability of the optics for simultaneously measuring the free-surface temperature and free-surface velocity. The free-surface temperature of aluminum 2024-T4 with a polished surface is in very good agreement with data in the literature as well as with simulations. Free-surface post-shock temperature measurements are very sensitive to the surface preparation. A rough surface produces micro-jets that can increase the measured free-surface temperatures by several 100 K. Also, rough surfaces are more likely to produce ejecta at higher temperatures than the free surface and corrupt the free-surface temperature measurement.

## REFERENCES


1. Raikes S.A. and Ahrens T.J., "Post-shock temperatures in minerals", Geophys. J. R. Astron. Soc. **58**, 717-747 (1979)
2. Yuan V.W. *et al.*, "Shock Temperature Measurement using Neutron Resonance Spectroscopy" Phys. Rev. Letters **94**, 125504 (2005)
3. Stewart S.T., "The Shock Compression Laboratory at Harvard: A New Facility for Planetary Impact Processes", Lunar and Planetary Science Conference XXXV, #1290, 2004
4. DeWitt D.P., Nutter G.D., *Theory and Practice of Radiation Thermometry* (John Wiley & Sons, New York, 1988).
5. Seifter A. *et al.*, "Low-temperature measurements on shock-loaded Tin", *Proceedings of High Speed Photography and Photonics 2004,* edited by D.L. Paisley, S. Kleinfelder, D.R. Snyder, B.J. Thompson, (Bellingham, WA, 2005), pp. 93-105
6. Steinberg, D. J., "Equation of State and Strength Properties of Selected Materials," Lawrence Livermore National Laboratory, UCRL-MA-106439, 1991.
7. McGlaun J.M. *et al.*, "CTH: A 3-dimensional shock-wave physics code", *Int. J. Impact Eng.*, *10*, 351-360 (1990).